Electronic Supplementary Information

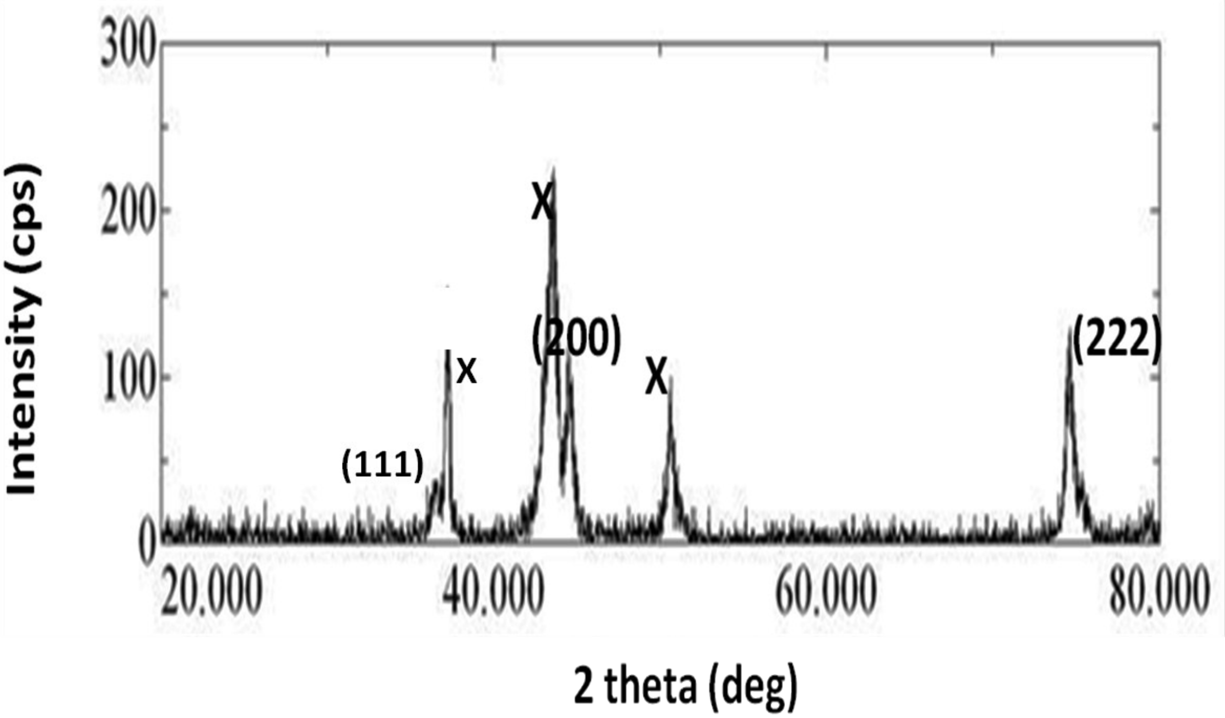

Fig. S1 XRD pattern of TiN coating

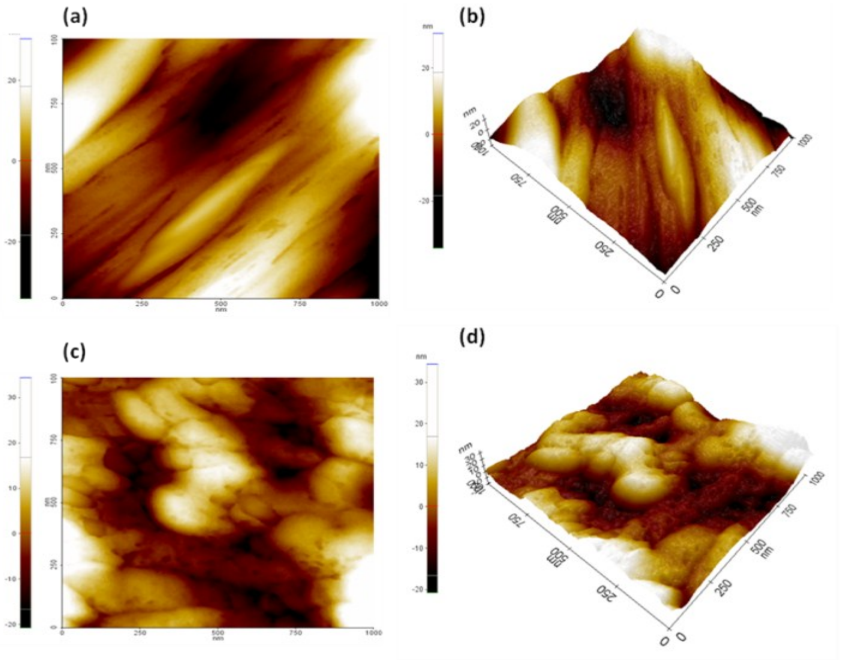

Fig. S2 The 2D & 3D AFM images for (a) & (b) uncoated, (c) & (d) for TiN coated 316L SS

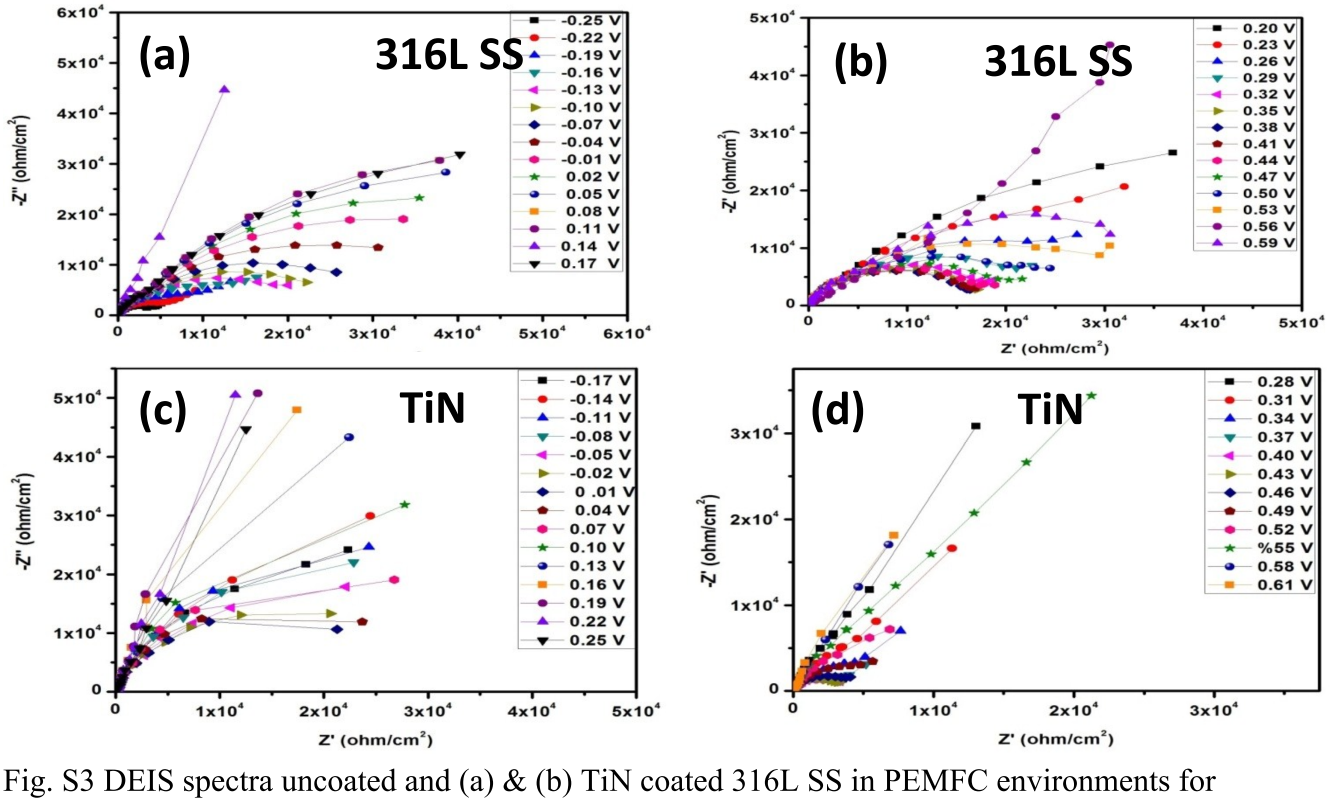

Fig. S3 DEIS spectra uncoated and (a) & (b) TiN coated 316L SS in PEMFC environments for (c) & (d)

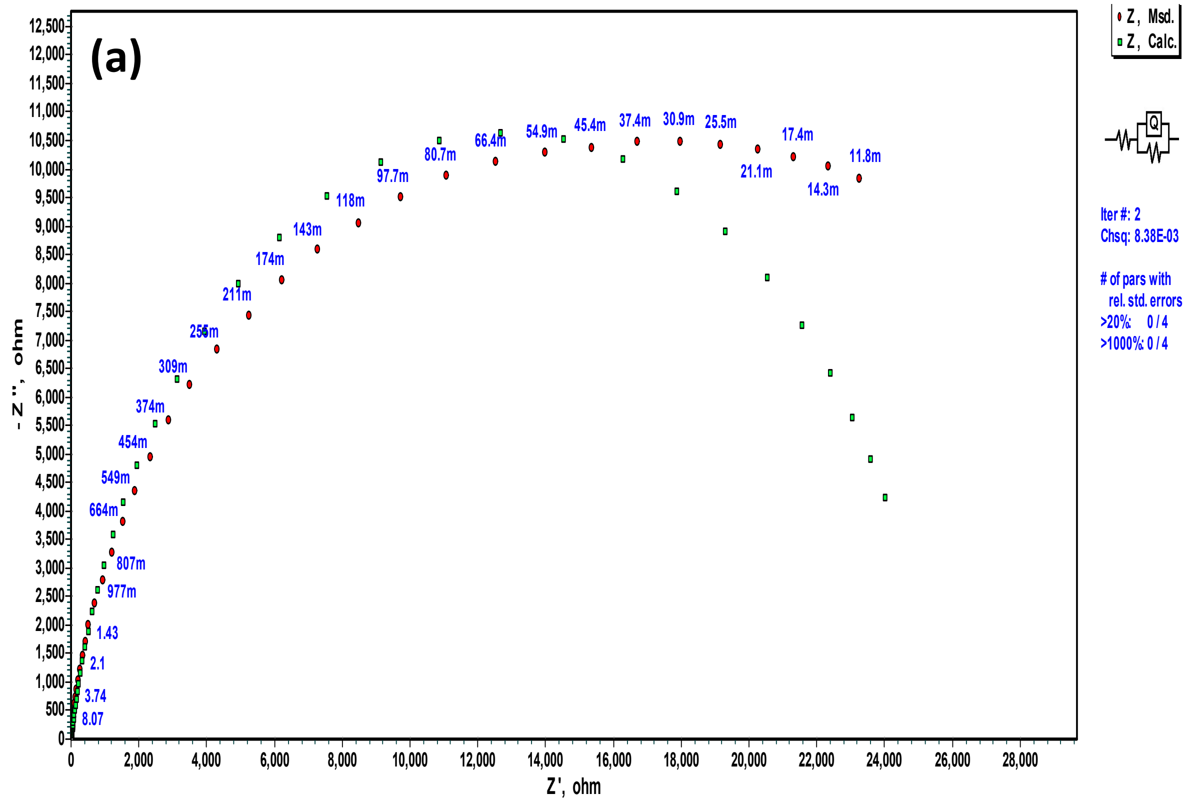
(a)
- Z '', ohm
Z', ohm
0
500
1,000
1,500
2,000
2,500
3,000
3,500
4,000
4,500
5,000
5,500
6,000
6,500
7,000
7,500
8,000
8,500
9,000
9,500
10,000
10,500
11,000
11,500
12,000
12,500
0
2,000
4,000
6,000
8,000
10,000
12,000
14,000
16,000
18,000
20,000
22,000
24,000
26,000
28,000
8.07
3.74
2.1
1.43
977m
807m
664m
549m
454m
374m
309m
255m
211m
174m
143m
118m
97.7m
80.7m
66.4m
54.9m
45.4m
37.4m
30.9m
25.5m
21.1m
17.4m
14.3m
11.8m
Z, Msd.
Z, Calc.
Q
Iter #: 2
Chsq: 8.38E-03
# of pars with
rel. std. errors
>20%: 0 / 4
>1000%: 0 / 4

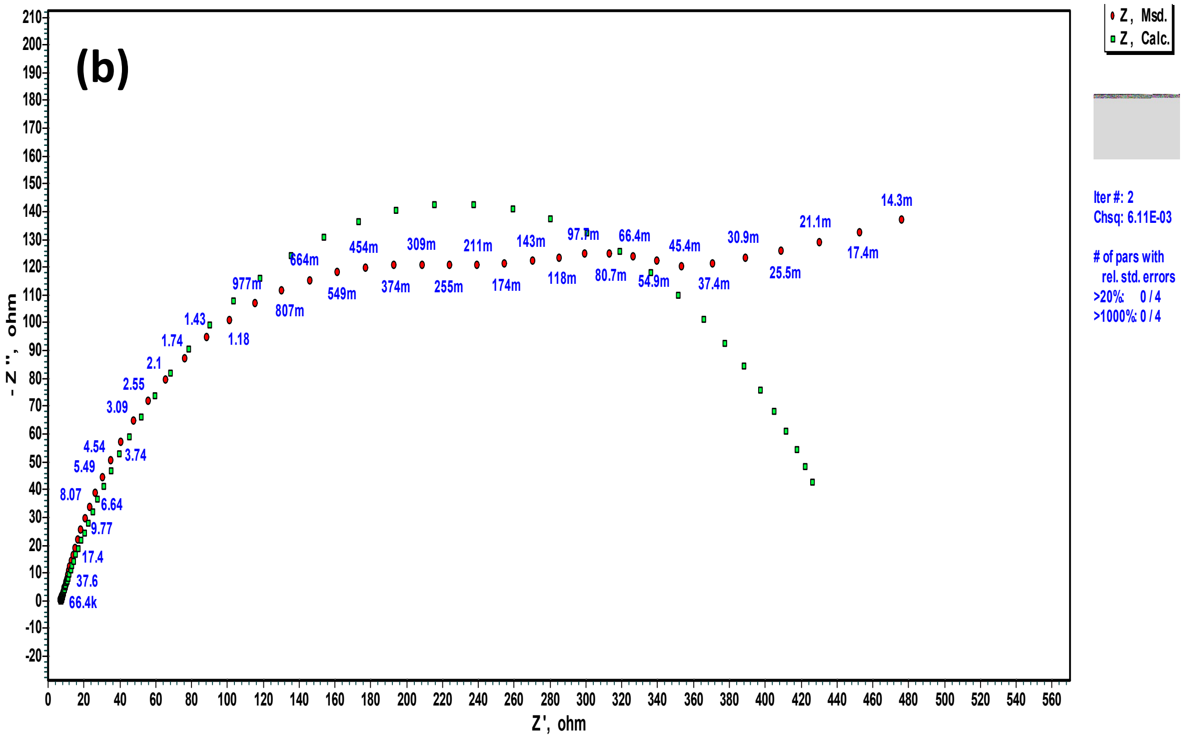
(b)
Z, Msd.
Z, Calc.
Iter #: 2
Chsq: 6.11E-03
# of pars with
rel. std. errors
>20%: 0 / 4
>1000%: 0 / 4
- Z '', ohm
Z', ohm
210
200
190
180
170
160
150
140
130
120
110
100
90
80
70
60
50
40
30
20
10
0
-10
-20
0
20
40
60
80
100
120
140
160
180
200
220
240
260
280
300
320
340
360
380
400
420
440
460
480
500
520
540
560
66.4k
37.6
17.4
9.77
8.07
6.64
5.49
4.54
3.74
3.09
2.55
2.1
1.74
1.43
1.18
977m
807m
664m
549m
454m
374m
309m
255m
211m
174m
143m
118m
97.7m
80.7m
66.4m
54.9m
45.4m
37.4m
30.9m
25.5m
21.1m
17.4m
14.3m

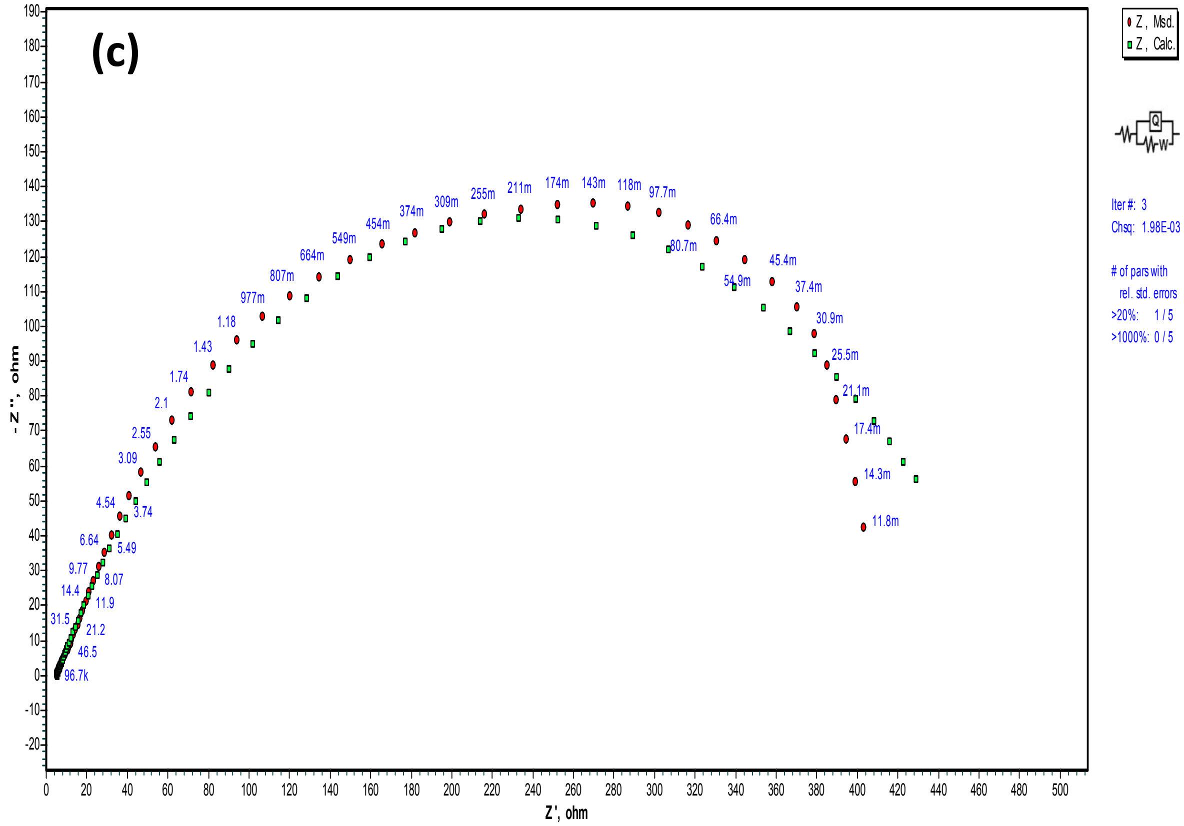
(c)
Z, Msd.
Z, Calc.
Iter #: 3
Chsq: 1.98E-03
# of pars with
rel. std. errors
>20%: 1 / 5
>1000%: 0 / 5
Q
W
- Z '', ohm
Z', ohm
190
180
170
160
150
140
130
120
110
100
90
80
70
60
50
40
30
20
10
0
-10
-20
0
20
40
60
80
100
120
140
160
180
200
220
240
260
280
300
320
340
360
380
400
420
440
460
480
500
96.7k
46.5
31.5
21.2
14.4
11.9
9.77
8.07
6.64
5.49
4.54
3.74
3.09
2.55
2.1
1.74
1.43
1.18
977m
807m
664m
549m
454m
374m
309m
255m
211m
174m
143m
118m
97.7m
80.7m
66.4m
54.9m
45.4m
37.4m
30.9m
25.5m
21.1m
17.4m
14.3m
11.8m

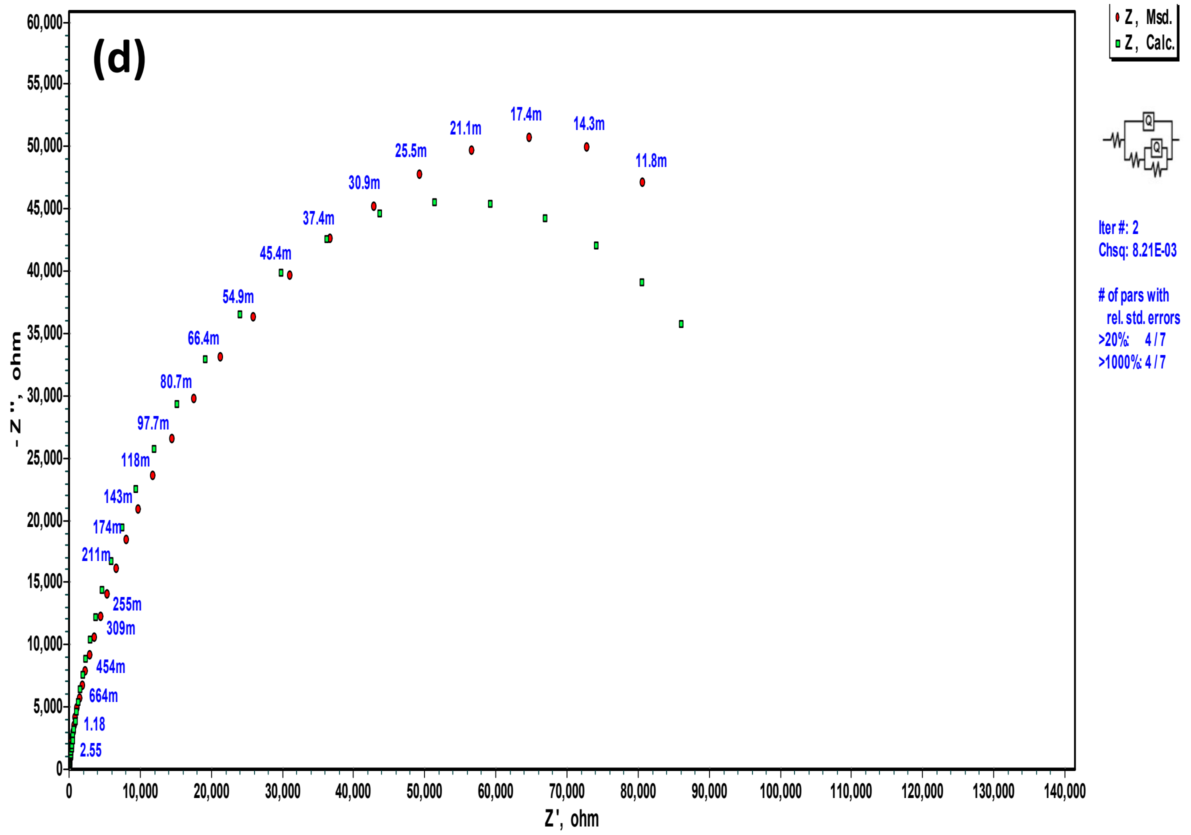
(d)
60,000
55,000
50,000
45,000
40,000
35,000
30,000
25,000
20,000
15,000
10,000
5,000
0
- Z '', ohm
0
10,000
20,000
30,000
40,000
50,000
60,000
70,000
80,000
90,000
100,000
110,000
120,000
130,000
140,000
Z', ohm
21.1m
17.4m
14.3m
25.5m
11.8m
30.9m
37.4m
45.4m
54.9m
66.4m
80.7m
97.7m
118m
143m
174m
211m
255m
309m
454m
664m
1.18
2.55
Z, Msd.
Z, Calc.
Iter #: 2
Chsq: 8.21E-03
# of pars with
rel. std. errors
>20%: 4 / 7
>1000%: 4 / 7

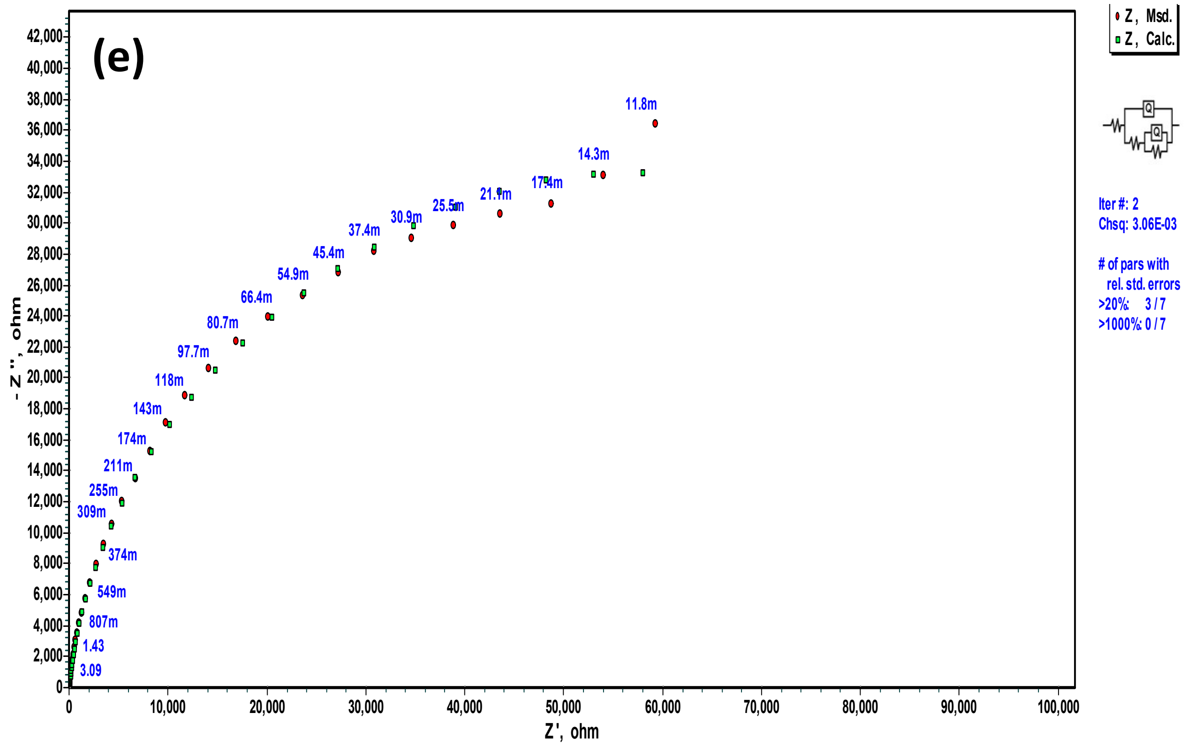
(e)
42,000
40,000
38,000
36,000
34,000
32,000
30,000
28,000
26,000
24,000
22,000
20,000
18,000
16,000
14,000
12,000
10,000
8,000
6,000
4,000
2,000
0
- Z '', ohm
0
10,000
20,000
30,000
40,000
50,000
60,000
70,000
80,000
90,000
100,000
Z', ohm
11.8m
14.3m
17.4m
21.1m
25.5m
30.9m
37.4m
45.4m
54.9m
66.4m
80.7m
97.7m
118m
143m
174m
211m
255m
309m
374m
549m
807m
1.43
3.09
Z, Msd.
Z, Calc.
Iter #: 2
Chsq: 3.06E-03
# of pars with
rel. std. errors
>20%: 3 / 7
>1000%: 0 / 7

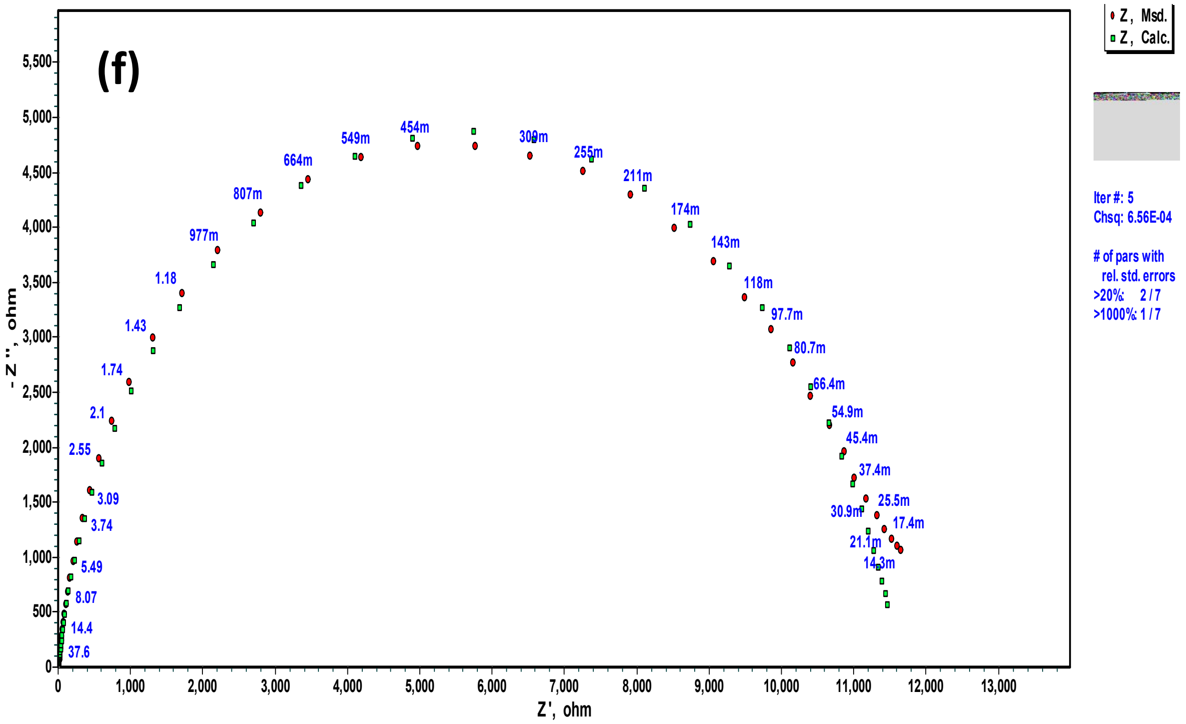

Fig. S4 EIS fitting analysis curves of uncoated and TiN coated 316L SS in all the environments

Table S1. EIS parameters obtained by equivalent circuits for uncoated and TiN coated 316L SS at OCP, PEMFC anode and cathode environments

Environment	**Material**	**R_s (Ω cm^2)**	**Q_{dl} (μF cm^{-2})**	**n_1**	**R_{ct} (Ω cm^2) × 10^4**	**Q_c (μF cm^{-2})**	**n_2**	**R_{coat} (Ω cm^2)**	**W ($S^{0.5}$ Ω^{-1} cm^{-2}) × 10^{-4}**	**χ^2 × 10^{-4}**
OCP	316L SS	1.4	7.30	0.85	5.187	-	-	-	-	8.38
	TiN	1.9	0.15	0.89	8.376	0.92	0.94	109.7	-	8.21
PEMFC Anode	316L SS	1.7	8.28	0.82	3.692	-	-	-	-	6.11
	TiN	2.3	0.72	0.87	6.099	0.98	0.91	101.3	-	3.06
PEMFC Cathode	316L SS	2.1	8.73	0.80	1.576	-	-	-	5.24	1.98
	TiN	1.7	0.91	0.86	5.279	1.43	0.89	91.2	-	0.65

R_s, $R_{ct,}$ R_{po}, Q_{dl} values were used to determine the corrosion resistance and surface conductivity of the uncoated and TiN coated 316L SS. The χ^2 values were obtained for both uncoated and TiN coated substrates were nearly approached 10^{-4} and listed in Table. S1 The fitted Nyquist plots were given in Fig. S4. A comparison of the R_{ct} values of the uncoated and TiN coated 316L SS at OCP, PEMFC anode and cathode conditions (Fig. 5e) revealed higher R_{ct} values for TiN coated substrate in each potential. With increasing potential, the values of R_{ct} decrease gradually for both uncoated and TiN coated substrates. The variation in R_{ct} values was related to the difference in operating potential (OCP. -0.1 V and 0.6 V) and environmental conditions. R_{coat} is decreased from OCP (109.7 Ω cm^2) to PEMFC anode (101.3 Ω cm^2) and cathode (91.2 Ω cm^2). These results clearly explained that the coating resistance decreases and surface conductivity increases with increasing potential in the coating/electrolyte interface. This might be probably due to the ion transport from the electrolyte to the coating. The capacitance of the TiN coated 316L SS increased from 0.92 to 0.98 $_{\mu F}$ cm^{-2} at OCP to PEMFC anode indicated decreased the corrosion resistance. Further, it was increased from 0.98 to 1.43 $_{\mu F}$ cm^{-2} at PEMFC anode to cathode. These results clearly demonstrated that the ions and charged species are entering into the coating in the cathode environment. The capacitance values related to the surface conductivity of TiN coating at the coating /electrolyte interface. Increased capacitance value with increasing potential is responsible for the increased surface conductivity of BP in the PEMFC environments. The highest capacitance value of the uncoated 316L SS could be attributed to the enhanced surface conductivity because of corrosion in the PEMFC cathode environment. At OCP, the double layer capacitance (Q_{dl}) values of the uncoated and TiN coated 316L SS for 7.30 and 0.15 $_{\mu F}$ cm^{-2}, respectively. It has increased from the OCP to PEMFC anode for both uncoated (8.28 $_{\mu F}$ cm^{-2}) and TiN coated 316L SS (0.72 $_{\mu F}$ cm^{-2}). Obviously, the higher Q_{dl} values for uncoated SS was related to the transformation of more charged species from the electrolyte solution to the substrate. The higher Q_{dl} value of uncoated 316L SS facilitates higher surface conductivity in the PEMFC anode environment. The highest Q_{dl} value obtained for uncoated 316L SS (8.73 $_{\mu F}$ cm^{-2}) in the PEMFC cathode environment indicates better charge transfer ability exhibiting enhanced surface conductivity and decreasing the corrosion resistance. The lower rate of Q_{dl} values for TiN coating (0.91 $_{\mu F}$ cm^{-2}) in the PEMFC cathode environment indicates higher charge transfer resistance at the substrate/electrolyte interface exhibiting enhanced corrosion resistance and decreasing the surface conductivity. The 'n' is denoted as a power of CPE in EIS analysis. At OCP, the n values of both uncoated and TiN coated 316L SS for 0.87 and 0.84, respectively, indicating both the substrates close to the ideal capacitive behavior **[56]**. The potential changed from the OCP to PEMFC anode, the n values of the both the substrates decreased. When the potential increases from PEMFC anode to cathode, the n value for uncoated 316L SS decreases from 0.85 to 0.82 and 0.80 at the substrate/electrolyte interface. It is attributed to the higher conductivity of uncoated 316L SS, thus facilitating the faster the degradation of passive film and resulting to the higher rate of corrosion. The n values of TiN coating showed much higher in all the environments at substrate/electrolyte and coating/electrolyte interfaces, which obviously improved the corrosion resistance and decreased the surface conductivity of BP in the PEMFC environments. Higher the Warburg resistance of the TiN coated substrate showed higher the tendency to control the ion diffusion process in a PEMFC cathode environment. Fig. S3(f) shows a declining trend in impedance behavior from 0.32 to 0.48 V for coated substrate than the uncoated one. This could be attributed to the pinholes formed because of corrosion by the influence of potential and environmental conditions. In the corresponding equivalent circuit (Fig, 5(d)). R_{coat} has been replaced by R_{pore} since penetration of corrosive ions takes place due to defects in the coating that have been formed during the deposition process. This is responsible for the decrease in impedance behavior from the potential region from 0.32 to 0.48 V for coated substrate than the uncoated 316L SS.

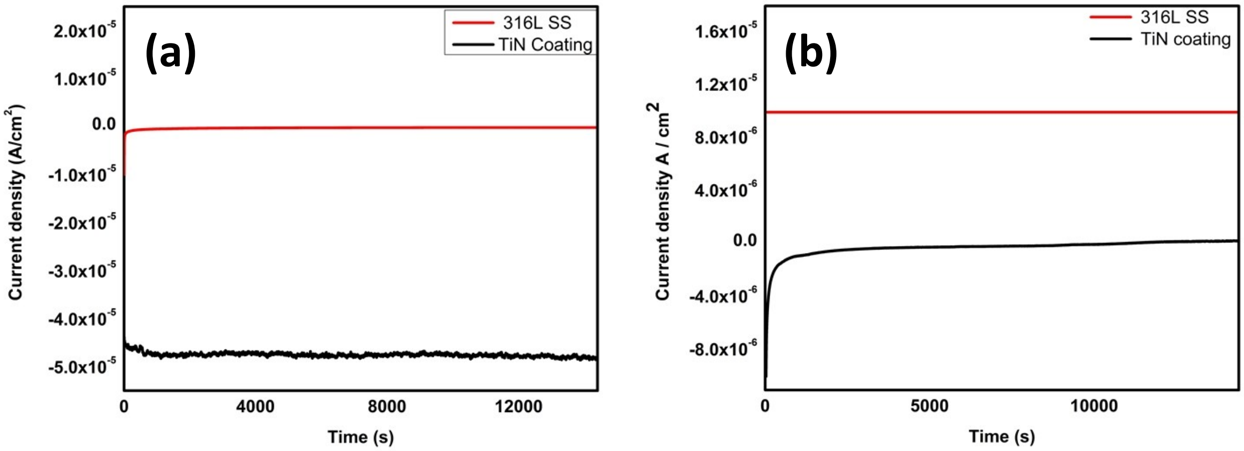

Fig. S5 Potentiostatic polarization curves of uncoated and TiN coated 316L SS in PEMFC (a) anode and (b) cathode environments.

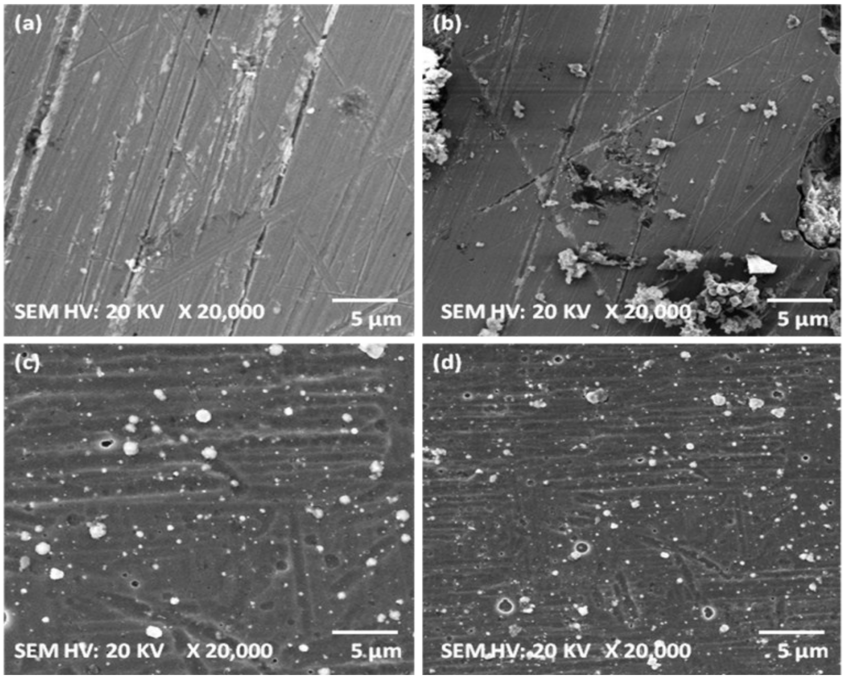

Fig. S6 SEM images for uncoated (a & b) and TiN coaed 316L SS (c & d) in PEMFC anode and cathode environments after polarization studies

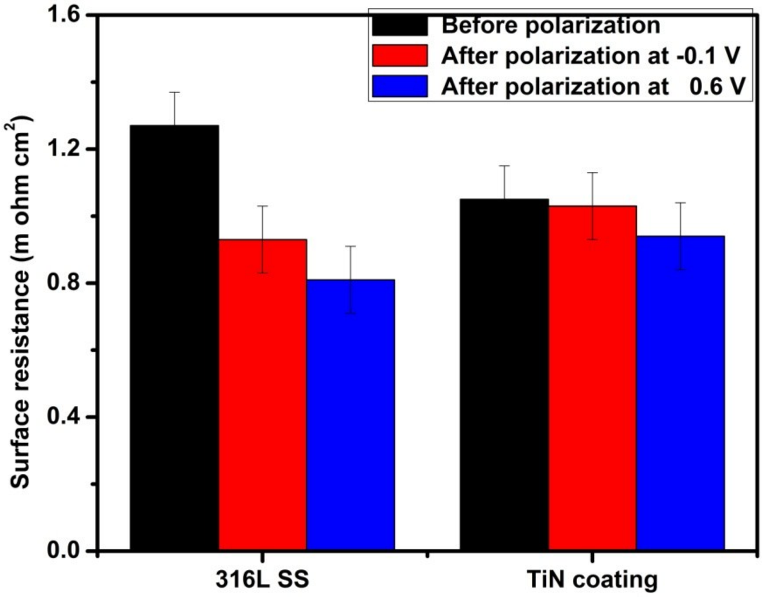

Fig. S7 Surface resistance measurements for uncoated and TiN coated 316L SS in before and after potentiostatic polarization studies

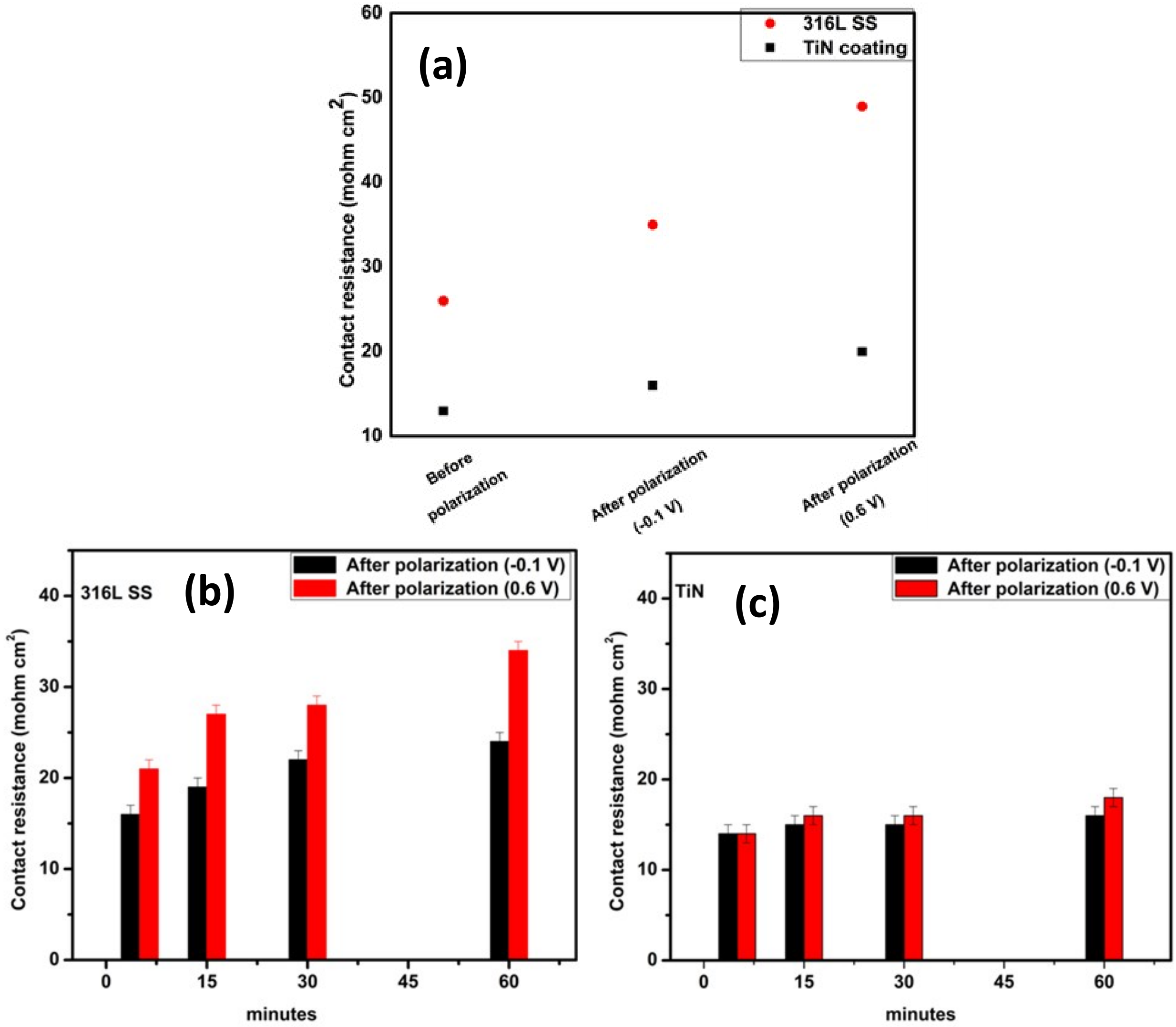

Fig. S8 (a) ICR values for uncoated and TiN coated 316L SS before polarization and after polarization at -0.1 V and 0.6 V, (b) & (c) Time vs ICR values of uncoated and TiN coated 316L SS at polarization at -0.1 V and 0.6 V